

## 論文の内容の要旨

# 論文題目 Optical Manipulation of Antiferromagnets (光による反強磁性体の制御)

氏名 樋口 卓也

### 1 Introduction

Recent developments in photonics have shed a new light on the vast, still unexplored nature of magnetism. For example, magneto-optical effects are widely employed to visualize the spatial distributions of magnetic domains, which underpin their well known applications in magnetic recording. Femtosecond laser pulses have recently revealed the dynamics of magnetism on a timescale even shorter than that of a single precession cycle. In addition, it has been demonstrated that light can even access a single spin, the smallest unit of magnetism; this is expected to work as a key element in quantum information and computation technologies. With the aid of optics, magnetism helps us to navigate our life in this era of modern informatics, and potentially of future quantum informatics – as magnetic compasses led the world to the Grand Navigations.

Among various magnets, we focus on two-sublattice antiferromagnets, a class of magnetic materials. The spins in their two types of sublattices are aligned opposite directions; they exhibit net no magnetic moment. This results in many attracting features. To name a few, antiferromagnetic domain boundaries are usually very thin, the typical domain size to sustain the magnetic order can be even a nanometer scale, and the spin dynamics in antiferromagnets are fast and have long coherence time. However, at the same time, the absence of magnetic moment has left them untamed, because their manipulation through an external field is quite formidable.

In this context, we propose that optical techniques pave a new way to manipulate antiferromagnetism. We demonstrate optical methods to control magnetic orders in  $\text{MnF}_2$  crystals and to manipulate magnetization dynamics in  $\text{NiO}$ ; both these materials are representative antiferromagnets. The key concepts for their realization are to fully employ space-time symmetry of the crystal and to tune the polarization state of the control lasers precisely.

### 2 Space-Time Symmetry of Optical Susceptibilities

This Chapter overviews symmetric relations of electromagnetics and crystals, mainly as a reference for our experimental and theoretical studies presented in the following Chapters. Neumann's principle suggests that every macroscopic property of a crystal possesses the symmetry described by the point group of the crystal. Another important rule is Onsager's reciprocity relations, which is a direct consequence of medium symmetry under time reversal. This explains Faraday rotation, where light propagating in a nonmagnetic medium under an external magnetic field experiences rotation of its polarization azimuth.

However, when the time reversal does not act as a symmetry operation of the crystal (in other words, if it is not *gray*), careful treatments of Onsager's relations are required. We show two approaches (1) employing a combined operation of a spacial operation and the time reversal (2) an explicit treatment of time-odd variables. In particular, the former is useful when the magnetic point group of the crystal is *black-and-white*. In these cases, unique magneto-optical effects, such as dichroism between two orthogonal linear polarizations under magnetic field, are allowed [1]. Note that  $\text{MnF}_2$  is an example of such materials.

### 3 Physical Properties of $\text{MnF}_2$

This Chapter describes a comprehensive survey of the structural, magnetic and optical properties of  $\text{MnF}_2$ . Main features in the optical spectrum of  $\text{MnF}_2$  in the visible region are dominated by  $d-d$  transitions in  $\text{Mn}^{2+}$  ions. The ground states of  $\text{Mn}^{2+}$  ions take high-spin  $d^5$  configurations; this makes the transitions spin-forbidden. Weak magnetic dipole transitions that directly create single ionic excitations are allowed by virtue of the spin-orbit coupling. In addition to these weak magnetic dipole transitions, much stronger electric dipole transitions were observed. This cannot be explained by single-ionic transitions, because electric dipole processes are parity-forbidden. In this Chapter, a mechanism proposed by Tanabe *et al.* that considers pair creations of excitons and magnons are reviewed. Optical absorption bands corresponding to this process are called magnon sidebands.

## 4 Selection Rules for Magneto-Optical Effects in MnF<sub>2</sub>

When an external magnetic field is applied along the  $c$  axis of a MnF<sub>2</sub> crystal, it is known that dichroism between two linear polarizations is induced, as discussed in Chapter 2. This dichroism is odd with respect to the external magnetic field and the antiferromagnetism vector; it is called magneto-linear dichroism (MLD). Two types of antiferromagnetic domains in MnF<sub>2</sub> [Fig. 1(a)] can be distinguished by this MLD. At the same time, magneto-circular dichroism (MCD) with a considerable strength was observed. A notifying feature of these MLD and MCD is that they have specifically different spectral shapes around the  ${}^6A_{1g} \rightarrow ({}^4A_{1g}, {}^4E_g)$  absorption line of Mn<sup>2+</sup>. As introduced in Chapter 1, one of our goals is to observe and manipulate antiferromagnetic domains in MnF<sub>2</sub>. Although these magneto optical phenomena are particularly important for this purpose, lack of systematic measurements of the dichroism prevailed comprehensive understandings of their origins.

We measured systematically the magnetic field dependence of these MLD and MCD of the  ${}^6A_{1g} \rightarrow ({}^4A_{1g}, {}^4E_g)$  lines [Fig. 1(b)] at 6 K. They are separated into two main features [Fig. 1(c)]: both MLD and MCD that originates from the magnetic dipole transition ( $M_\pi$ ), and the presence of a strong MLD and the absence of MCD at the edges of the magnon sideband ( $E_{2\sigma}^{(\text{high})}$  and  $E_{2\sigma}^{(\text{low})}$ ). We clarified that additional conditions restrict the dichroism when the cubic crystal field is much stronger than the spin-orbit coupling. This explains the reason why only significant MLD was observed for the magnon sideband. These experimental observations matched well with the calculated spectra of MLD and MCD considering dispersions of magnons and excitons [Figs. 1(e), (f), and (g)].

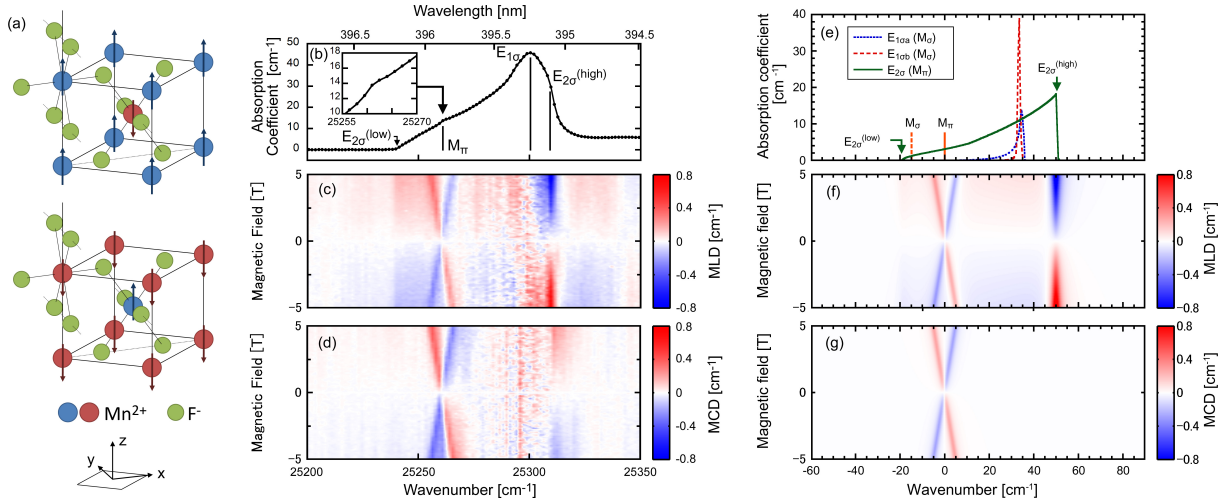


Figure 1: (a) Crystal and spin structure of two types of antiferromagnetic domains in MnF<sub>2</sub>. (b) Absorption coefficient of MnF<sub>2</sub> for light propagating along its  $c$  axis. Experimental spectra of (c) MLD between  $x$  and  $y$  polarizations and (d) MCD. Calculated spectra of (e) optical absorption (f) MLD, and (g) MCD.

## 5 Optical Manipulation of Antiferromagnetic Domains

Just below the Néel temperature (67 K) of MnF<sub>2</sub>, this crystal shows MLD, whose sign depends on the sign of the antiferromagnetic order parameter [Fig. 2(a)]. We observed spatial distributions of domains by means of this MLD. This MLD can also introduce an imbalance between the forming energies of two different antiferromagnetic domains when the crystal is optically pumped by an intense linearly polarized laser under a magnetic field. We employed this imbalance to control boundaries of antiferromagnetic domains in MnF<sub>2</sub>, as shown in Fig. 2(b). The position of the boundary depended on the polarization azimuth of the pump beam, which clearly indicates that the controlling mechanism is polarization-dependent optical pumping [Fig. 2(c)]. Wide varieties of applications are expected, such as formation of artificially frustrated antiferromagnets via optical patterning.

## 6 Dynamics of Magnetism Excited by Optical Pulses

Ultrafast control of magnetization via impulsive stimulated Raman scattering (ISRS) has recently attracted considerable interest. In Chapter 6, we describe a phenomenological theory for excitation of magnons in

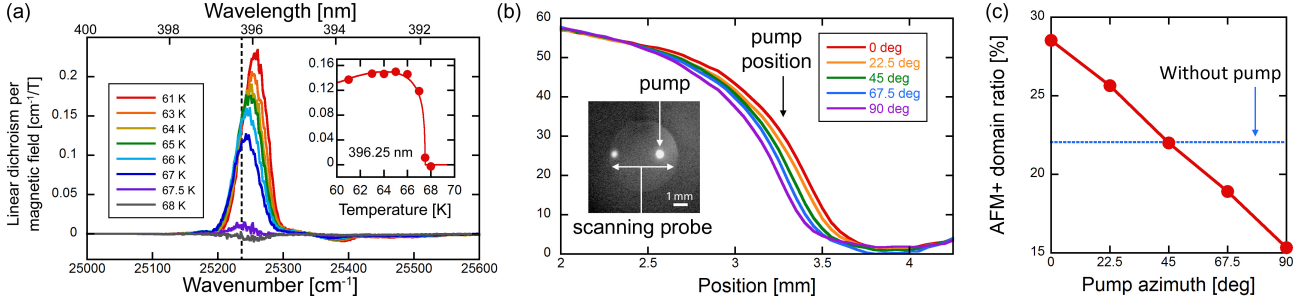


Figure 2: (a) MLD spectra of a single domain  $\text{MnF}_2$  around its Néel temperature. Inset shows the temperature dependence of MLD for an optical wavelength of 396.25 nm. This wavelength was employed for both observation and manipulation of antiferromagnetic domains. (b) Line profile of the domain distribution. Different curves show the distributions under pumping by lasers with different azimuthal angles. (c) Change of the domain population at the pump position as a function of the pump laser azimuth.

$\text{NiO}$  by ISRS. This is formulated by the modulation of the optical susceptibility tensor under presence of magnons. Since  $\text{NiO}$  has a *gray* magnetic point group, optical susceptibility should be even functions of the antiferromagnetism vector; this is important to determine the form of its susceptibility tensor. As a result, both circular and linear polarizations are found to contribute magnon excitation. There exist clear selection rules between the polarization states, and the modes and phases of the excited magnon modes. Methods to observe the induced magnons are also discussed.

## 7 Ultrafast Optomagnetism along a Threefold Axis

When the crystal has a uniaxial optical axis, the selection rules for ISRS be simplified by means of conservation laws of angular momentum [Fig. 3(a)]. Chapter 7 describes this simplified polarization selection rule for a light induced magnetization dynamics in  $\text{NiO}$ . Here, the role of discrete rotational symmetry of the crystal is clarified. When a fundamental light beam propagates along a continuous rotational axis, magnetization can only be induced along that axis [Fig. 3(b)], while generation of magnetization in the perpendicular plane is prohibited. One method to control such in-plane magnetization is to employ a linearly polarized laser pulse propagating along a threefold rotational axis of a crystal. With such geometry, the rotational analogue of the umklapp process allows a change of the angular momentum of the light field and induced magnetization by  $\pm 3\hbar$  [2]. This activates the otherwise forbidden path to access in-plane magnetization by ISRS and subsequent difference-frequency generation (DFG) [Figs. 3(c) and (d)]. As a demonstration, we observed radiation ( $\sim 1$  THz) from the magnetic oscillations induced by linearly polarized laser pulses along a  $[111]$  axis of a single crystal of antiferromagnetic  $\text{NiO}$  with micro multi-domain structure [Figs. 3(e), (f), and (g)]. Clear polarization dependence on the incident and the radiated photons was obtained [Fig. 3(h)], which agreed excellently with the theoretical prediction.

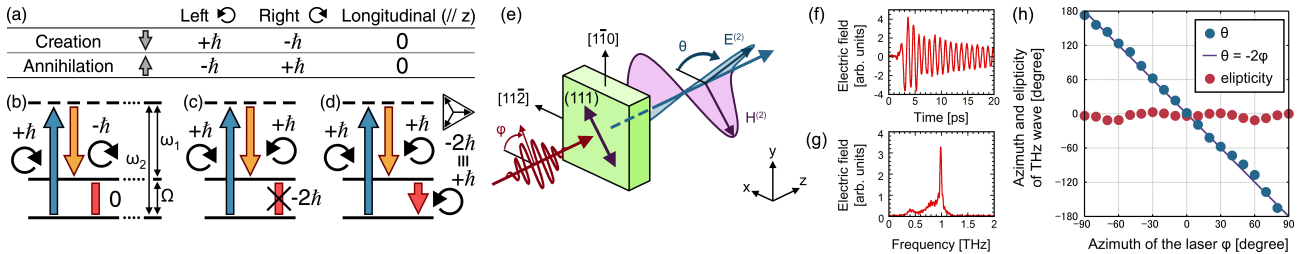


Figure 3: (a) Changes in angular momenta of the electromagnetic fields by creation or annihilation of photons propagating along the  $z$ -axis. The lower panels show schematics of the changes of the angular momentum in collinear scattering processes of photons to a mode with (b) the same helicity and (c) the opposite, and (d) a collinear DFG process allowed along a threefold axis involving two photons with opposite helicity. (e) Schematics of the experimental setup, (f) temporal waveform of the terahertz waves radiated from  $\text{NiO}$  and (g) their Fourier transformed spectrum. (h) Ellipticity and azimuth  $\theta$  of the radiated waves as functions of the pump azimuth  $\varphi$ , together with a theoretical line  $\theta = -2\varphi$  [3].

## 8 Envelope Helicity and the Vectorial Manipulation of Magnetization

In this Chapter, we discuss a general approach for controlling low-energy rotational excitations by ISRS [4]. ISRS is free from thermalization, because the scattered light carries away the excess energy [Fig. 4(a)]. A femtosecond pulse is employed because it has a broadband spectrum that covers the needed frequencies in a single pulse [Fig. 4(b)]. However, a design for a continuous spectrum in nonlinear process usually imposes a complex analysis of the electromagnetic and material parameters. This is because ISRS is intrinsically a two-photon process, and one photon can contribute to multiple scattering processes. Therefore, independent optimization of polarization states of each frequency component is no more a good strategy. Here, we theoretically show that the temporal trajectory of the envelope of the electromagnetic-field vector [Fig. 4(c)] enables us to intuitively interpret ISRS experiments and optimize the controlling laser pulse. To describe the envelope of a light pulse, instantaneous Stokes parameters (ISP) are defined under slowly varying envelope approximation. Envelope helicity is introduced to the Fourier component of the ISPs, which determines the change of angular momentum via ISRS. As an application, we employ this concept to interpret the vectorial manipulation of magnetization in an antiferromagnetic NiO [5].

This opens new routes to design experiments to manipulate low-energy rotational excitations in ultrafast timescales; not by simple heating and demagnetization effect, but rather by much more interesting phenomena based on coherent nonlinear optical transitions and material symmetries.

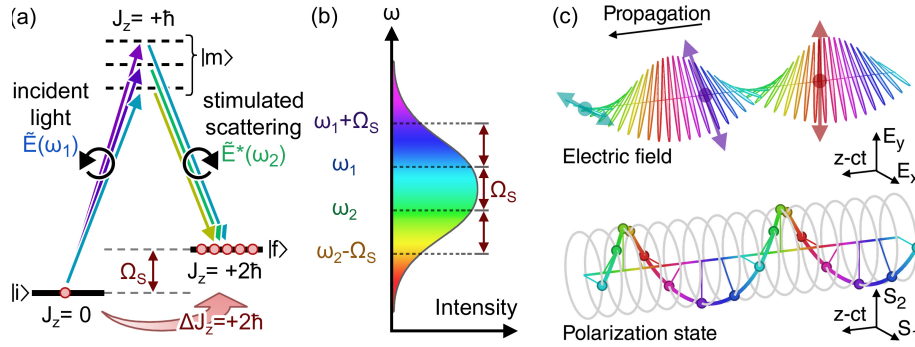


Figure 4: (a) Schematics of ISRS. A photon ( $\tilde{E}(\omega_1)$ ) is scattered to a different mode ( $\tilde{E}^*(\omega_2)$ ). The electronic system is transferred from the initial state ( $|i\rangle$ ) to the final state ( $|f\rangle$ ) via virtual intermediate states ( $|m\rangle$ ). (b) Spectrum of a femtosecond pulse that covers pairs of frequencies needed for ISRS. (c) An example of a light pulse that selects angular momentum transfer via ISRS. Top panel plots electric field, while bottom panel shows two components ( $S_1$  and  $S_2$ ) of the ISPs representing polarization azimuth.

## 9 Concluding remarks

In summary, we demonstrated novel methods to manipulate antiferromagnets by employing space-time symmetry of the crystals and tuning azimuthal angles of linearly polarized lasers. This study covers interactions between light and magnetism in specific materials, i. e.,  $\text{MnF}_2$  and NiO. It is worth unifying these two cases, under a single framework. Roughly speaking, the key concept unifying our results is the similarity of antiferromagnets and linearly polarized light in that angular momentum is canceled between their two degenerate constituents. It is widely believed that circularly polarized light is favorable for optical control of magnetism because such light carries spin angular momentum. On the other hand, a linearly polarized light contains same populations of left and right circularly polarized components, and their spin angular momenta are canceled. This is the reason why its abilities to control magnetism have been usually put aside. However, we showed that the relative phase between the two circular components, i. e., the polarization azimuth, plays a key role to manipulate antiferromagnets through selection rules based on the space-time symmetry of the crystal.

## References

- [1] V. V. Eremenko and N. F. Kharchenko, Phys. Rep. **155**, 379 (1987).
- [2] H. J. Simon and N. Bloembergen, Phys. Rev. **171**, 1104 (1968).
- [3] T. Higuchi, N. Kanda, H. Tamaru, and M. Kuwata-Gonokami, Phys. Rev. Lett. **106**, 047401 (2011).
- [4] Y.-X. Yan, J. Edward B. Gamble, and K. A. Nelson, J. Chem. Phys. **83**, 5391 (1985).
- [5] N. Kanda, T. Higuchi, H. Shimizu, K. Konishi, K. Yoshioka, and M. Kuwata-Gonokami Nat. Commun. **2**, 362 (2011).